PROCEEDINGS, 43rd Workshop on Geothermal Reservoir Engineering
Stanford University, Stanford, California, February 12-14, 2018
SGP-TR-213

# High Efficiency and Large-scale Subsurface Energy Storage with $CO_2$

Mark R. Fleming[1], Benjamin M. Adams[2], Jimmy B. Randolph[1,3], Jonathan D. Ogland-Hand[4], Thomas H. Kuehn[1], Thomas A. Buscheck[3], Jeffrey M. Bielicki[4], Martin O. Saar*[1,2]

[1]University of Minnesota, Minneapolis, MN, USA; [2]ETH-Zurich, Zurich, Switzerland; [3]TerraCOH Inc., Minneapolis, MN, USA; [4]The Ohio State University, Columbus, OH, USA; [5]Lawrence Livermore National Laboratory, Livermore, CA, USA.

*Corresponding Author: saarm@ethz.ch

**Keywords:** geothermal energy, multi-level geothermal systems, sedimentary basin, carbon dioxide, electricity generation, energy storage, power plot, CPG

## ABSTRACT

Storing large amounts of intermittently produced solar or wind power for later, when there is a lack of sunlight or wind, is one of society's biggest challenges when attempting to decarbonize energy systems. Traditional energy storage technologies tend to suffer from relatively low efficiencies, severe environmental concerns, and limited scale both in capacity and time.

Subsurface energy storage can solve the drawbacks of many other energy storage approaches, as it can be large scale in capacity and time, environmentally benign, and highly efficient. When $CO_2$ is used as the (pressure) energy storage medium in reservoirs underneath caprocks at depths of at least ~1 km (to ensure the $CO_2$ is in its supercritical state), the energy generated after the energy storage operation can be greater than the energy stored. This is possible if reservoir temperatures and $CO_2$ storage durations combine to result in more geothermal energy input into the $CO_2$ at depth than what the $CO_2$ pumps at the surface (and other machinery) consume. Such subsurface energy storage is typically also large scale in capacity (due to typical reservoir sizes, potentially enabling storing excess power from a substantial portion of the power grid) and in time (even enabling seasonal energy storage).

Here, we present subsurface electricity energy storage with supercritical carbon dioxide ($CO_2$) called $CO_2$-Plume Geothermal Energy Storage (CPGES) and discuss the system's performance, as well as its advantages and disadvantages, compared to other energy storage options. Our investigated system consists of a deep and a shallow reservoir, where excess electricity from the grid is stored by producing $CO_2$ from the shallow reservoir and injecting it into the deep reservoir, storing the energy in the form of pressure and heat. When energy is needed, the geothermally heated $CO_2$ is produced from the deep reservoir and injected into the shallow reservoir, passing through a power generation system along the way. Thus, the shallow reservoir takes the place of a storage tank at the surface. The shallow reservoir well system is a huff-and-puff system to store the $CO_2$ with as few heat and pressure losses as possible, whereas the deep reservoir has an injection and a production well, so the $CO_2$ can extract heat as it passes through.

We find that both the diurnal (daily) and seasonal (6 months) CPGES systems generate more electricity to the power grid than they store from it. The diurnal system has a ratio of generated electricity to stored electricity (called the Energy Storage Ratio) between 2.93 and 1.95. Similarly, the seasonal system has an energy storage ratio between 1.55 and 1.05, depending on operational strategy. The energy storage ratio decreases with duration due to the pump power needed to overcome the increasing reservoir pressures as $CO_2$ is stored.

## 1. INTRODUCTION

The development of modern electricity systems which reduce the amount of carbon dioxide ($CO_2$) emitted into the atmosphere while producing steady, continuous power is one of society's biggest challenges. To limit the global mean temperature rise to 2°C, the Intergovernmental Panel on Climate Change (IPCC) has estimated that an atmospheric limit of 250 ppm of $CO_2$ results in a 50% chance of obtaining this temperature goal (IPCC 2014a). These regulations were agreed upon by a majority of nations in the Paris Agreement (United Nations Framework Convention on Climate Change 2015), allowing for an estimated 1000 GT of $CO_2$ to be emitted after 2011 (IPCC 2014b). This requires the immediate reduction, and eventual elimination of $CO_2$ emissions, to avoid exceeding this $CO_2$ emission limit. No single technology will provide the necessary reduction and elimination of $CO_2$ emissions; however, multiple technologies employed and integrated as a whole can provide the necessary reduction in $CO_2$ emissions. To reduce $CO_2$ emissions in the electricity sector, which accounts for 25% of the total $CO_2$ emissions, existing power plants can be retrofitted with $CO_2$ capture technologies and carbon-neutral power systems can replace existing generation (IPCC 2014a; Metz et al. 2005).

To decarbonize existing power plants, $CO_2$ emissions can be captured, transported, typically via a pipeline, to a storage site, and then injected into a subsurface reservoir, in a process referred to Carbon Capture and Storage (CCS). CCS reduces the emission of $CO_2$ into the atmosphere from sources such as fossil fuel power systems, cement factories, biofuel refineries, or from other large $CO_2$ point sources by permanently storing the $CO_2$ underground in deep saline aquifers or partially depleted oil/gas fields, which can store large volumes of $CO_2$. The vertical leakage of the captured $CO_2$, which is naturally buoyant at the storage conditions, is contained by the overlying low permeability caprock. In addition to structural trapping, $CO_2$ is stored in the reservoir due to capillary forces, dissolution into the underlying brine, and eventually the formation of carbonate minerals. Due to the depth of the storage formation, which is generally in excess of 800 meters to ensure supercritical $CO_2$ and maximize storage volumes, the average reservoir temperatures are greater than the temperature of the injected $CO_2$, and can be significantly greater, depending on the geothermal gradient, than the surface temperature, thus allowing the injected $CO_2$ to extract heat from the reservoir. This heat extraction process has led to the proposal of geothermal energy systems which can be combined with CCS, such as $CO_2$-Plume Geothermal (CPG), which directly uses the $CO_2$ as the heat extraction fluid, thereby operating as a Carbon Capture Utilization and Storage (CCUS) system, discussed in detail below.

In addition to CCS, renewable energy sources, such as wind and solar, can provide energy without fossil fuels, and their associated $CO_2$ emissions; however, these sources are variable power systems, capable of producing power only when the given resources are available. In 2016, wind had an annual capacity factor of 34.5%, while solar photovoltaic had a 25.1% capacity (EIA 2017), due to the variability of their resources. The intermittent nature of these resources can provide challenges integrating these technologies into existing electrical grids by creating an excess or deficit in power generation, reducing the efficiency of the grid (Bird et al. 2013; Phuangpornpitak and Tia 2013). To provide baseload power, energy storage systems can be integrated with the intermittent renewable sources to store excess power when it is generated, producing the energy at a later period when there is a demand for power (Koohi-Kamali et al. 2013; Sørensen 2015). With the expanded capacity of wind and solar, additional energy storage capacity is required to ensure electrical grid reliability. However, existing large-scale bulk energy storage systems, such as Pumped Hydroelectric and Compressed Air, may not have the ability to provide the expanded capacity that is required. Pumped Hydroelectric systems, have limited development opportunities resulting from environmental concerns regarding the development of the large surface storage reservoirs. Additionally, compressed air does not represent a sustainable long-term energy storage solution, as compressed air relies on auxiliary surface heating, typically from natural gas, to produce power, emitting $CO_2$ in the process. While these energy storage technologies have limitations, geothermal energy is widely available and can be accessed by $CO_2$-Plume Geothermal systems, which can be used to supplement wind and solar.

$CO_2$-Plume Geothermal (CPG) systems operate by producing hot $CO_2$, which is geothermally heated in a natural high permeability reservoir, to the surface for power, or heat, generation (Adams et al. 2014, 2015, Randolph and Saar 2011a, 2011b, 2011c). The produced $CO_2$ is then reinjected into the reservoir, in a cold dense state, allowing the injected $CO_2$ to extract heat from the reservoir. CPG is different than $CO_2$-Enhanced Geothermal Systems ($CO_2$-EGS), which have previously been studied (Atrens et al. 2009, 2010; Brown W. 2000; Pruess 2008), as the CPG system uses natural high permeability sedimentary basins with a large storage volume, whereas $CO_2$-EGS requires artificially generated high permeability reservoirs which are generally small and offer limited $CO_2$ storage capacity.

Operating a geothermal power system using $CO_2$ has several advantages, beyond the synergistic power production from a CCS site, including a low mineral solubility, high reservoir mobility (low kinematic viscosity), and a large density variation with temperature. A low mineral solubility is advantageous, as the produced fluid will contain minimal impurities and pipe scaling will be limited. A low kinematic viscosity increases the mobility of the $CO_2$ in the reservoir, allowing the fluid to move through the reservoir and extract heat, with reduced pressures losses. The larger variation in the density with temperature allows a geothermal system to operate with a thermosiphon, which is naturally occurring convective circulation of the $CO_2$ to the surface, which reduces or eliminates the need for pumps. This is achieved by extracting hot low-density $CO_2$ from the reservoir, cooling it at the surface, and then injecting cold dense $CO_2$ into the reservoir, utilizing the density difference in each vertical well to create a pressure difference, thereby reducing or eliminating the need for circulation pumps in the system.

In this paper, we demonstrate how a CPG system can be modified to operate as a $CO_2$-Plume Geothermal Energy Storage (CPGES) system, storing energy over both diurnal and biannual periods, using a multi-reservoir approach, for a small demonstration-sized plant, operating with $CO_2$-plume sizes consistent with previous work (Adams et al. 2014, 2015, Garapati et al. 2014, 2015). The CPGES system differs from previously proposed $CO_2$ based energy storage systems which include the $CO_2$-Bulk Energy Storage System ($CO_2$-BES) and the Compressed $CO_2$ systems. The $CO_2$-BES produces and stores energy using a multi-fluid approach using multiple concentric circular horizontal wells, where $CO_2$ is used as a cushion gas, displacing brine and increasing the reservoir pressure to produce brine without downhole circulation pumps (Buscheck et al. 2016). The compressed $CO_2$ system is similar the proposed CPGES system, using multiple reservoirs to time shift generation and consumption, however, the geothermal energy is used to pre-heat the fluid, with the majority of the heat added at the surface from a fuel source (Liu et al. 2016).

## 2. SYSTEM OVERVIEW

The CPG system consists of injection and production wells, and a surface plant to convert the extracted heat into electrical power at the surface, and a permeable sedimentary reservoir which is overlain by a low-permeability caprock (Randolph and Saar 2011a, 2011b, 2011c). To produce power, the surface plant can directly expand the $CO_2$ in a turbine or operate as a binary system in which the $CO_2$ is used to heat a secondary working fluid to produce power, however, the direct CPG system typically produces more power (Adams et al. 2015), and thus we only consider the direct CPG system here. In the direct system, $CO_2$ is extracted from the reservoir and produced at the surface in a vertical well. At the surface, $CO_2$ is directly expanded in a turbine, generating electrical energy, and is then subsequently cooled using wet cooling towers, increasing the density of the $CO_2$ for reinjection into the reservoir. After the cooling process, the $CO_2$ may be compressed using a circulation pump and then further compressed down the injection well to the reservoir. In the reservoir, the cold, dense $CO_2$ extracts heat as the $CO_2$ plume expands and moves away from the injection well. For the direct system, a circulation pump is not required to operate, as the system can operate using only a thermosiphon, however, a circulation pump increases the net power generation of the system (Adams et al. 2014, 2015).

The CPG system can be modified to operate as an energy storage system by adding a second shallow reservoir to store the $CO_2$ in an intermediate state after the turbine, but before the parasitic loads, separating the components which generate and consume power, illustrated in Figure 1. The $CO_2$-Plume Geothermal Energy Storage (CPGES) system operates using two modes:

1. **Power Generation**: Hot $CO_2$ is produced from the deep reservoir and brought to the surface in the vertical production well, and expanded in the turbine to produce power. After the turbine, the $CO_2$ is partially cooled only to the extent necessary to be stored in the shallow reservoir. With increased density, the $CO_2$ is injected into the shallow reservoir using only the gravitational compression in the vertical well. The shallow reservoir stores the $CO_2$ until the end of the generation mode.

2. **Energy Storage**: $CO_2$ is produced from the shallow reservoir and brought to the surface through the same vertical well, it is then cooled using cooling towers, compressed using a pump, and injected back into the deep reservoir through the vertical injection well.

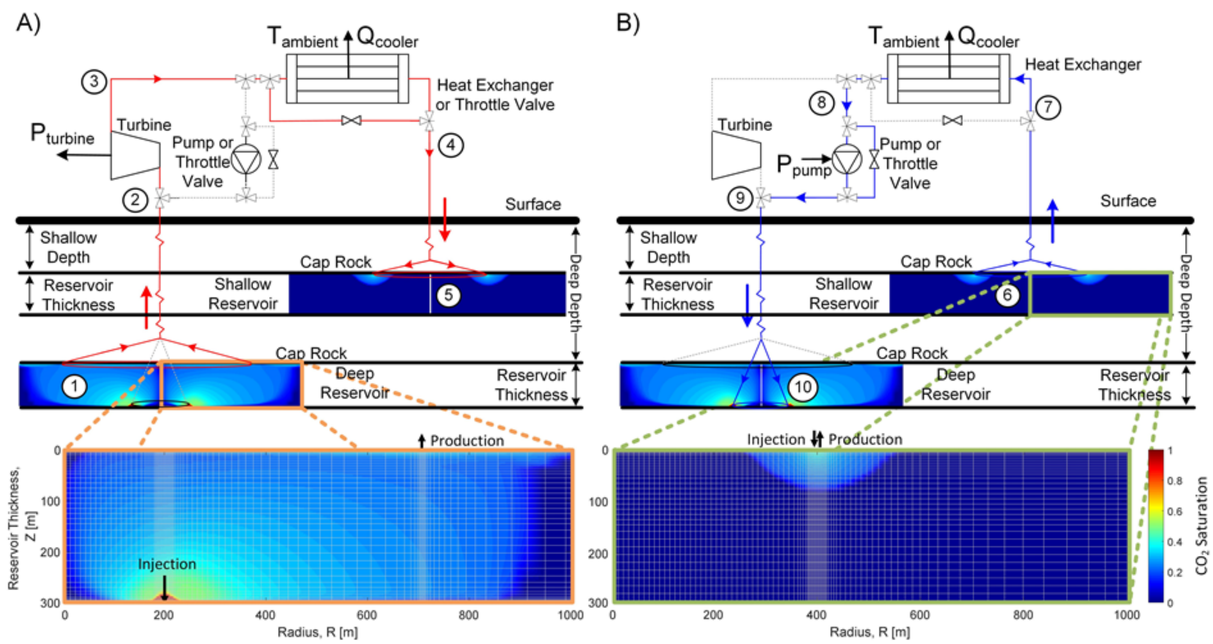


**Figure 1: The CPGES system operates using two modes: A) Power generation where the system produces net power to the electrical grid and B) Energy Storage where the system consumes electrical power to cool and compress the $CO_2$. Power is produced by extracting $CO_2$ from the shallow reservoir to the surface, expanded in a turbine to produce power, partially cooled, and injected into a shallow, storage reservoir. To consume power the system extracts $CO_2$ from the shallow reservoir and produces it at the surface, where it is cooled and compressed before it is injected back into the deeper reservoir where the $CO_2$ is heated, extracting energy from the reservoir. The operation of each reservoir is the system is different and requires each reservoir to operate with an independent configuration. The shallow reservoir operates using a single well, which operates as both the injection and production well. The deeper reservoir, the thermal source for the system, operates with two horizontal-circular wells, allowing heat to be extracted from a significant portion of the reservoir. The $CO_2$ plume in each reservoir, with the computational grid overlaid, is displayed below the system diagram. The deep reservoir requires a significant $CO_2$ plume for operation, where the shallow reservoir operates using limited $CO_2$.**

The CPGES system, like the CPG system, is a Rankine power cycle fueled by geothermal heat. As the CPGES system is a power cycle, the system generates more net energy to the grid than it consumes from the grid, due to the addition of the geothermal heat from the deep reservoir. Similarly, compressed air energy storage systems also generate more power to the grid than they consume, but they do this by combusting fossil fuel, emitting $CO_2$. Thus, the CPGES system operates using geothermal energy, producing net power to the grid without $CO_2$ emissions.

## 3. SYSTEM MODELING

We simulate the CPGES system using two separate models: the subsurface geologic reservoirs and a surface power plant. The subsurface power plants are simulated using TOUGH2 (Pruess et al. 2012) with the ECO2N (Pruess 2005) equation of state and the surface power plant is modeled using Engineering Equation Solver (EES) (Klein and Alvarado 2002). We use two storage cycles: a diurnal cycle with power generation occurring for 16 hours and energy storage occurring for the remaining 8 hours, and a seasonal storage model, with a continuous power generation period followed by a continuous energy storage period, each operating for 3 months.

### 3.1 Reservoir Modeling

We numerically simulate each reservoir employing a three-dimensional, axisymmetric geometry, illustrated in Figure 1. Each model is bounded by an impermeable caprock above and bedrock below. To avoid boundary effects, the models are simulated out to a radius of 100 km, similar to prior reservoir models (Garapati et al. 2015). Modeled reservoir properties are given in Table 1.

**Table 1: Reservoir physical properties for the numerical simulation.**

| Reservoir Parameter/Value | | | |
|---|---|---|---|
| **General Properties** | | **Deep Reservoir** | |
| Horizontal Permeability | 5.0 x $10^{-14}$ $m^2$ | Mean Reservoir Depth | 2.5 km |
| Vertical Permeability | 2.5 x $10^{-14}$ $m^2$ | Mean Reservoir Temperature | 102.5 °C |
| Thermal Conductivity | 2.1 W/m/°C | Injection Well Radius | 200 m |
| Porosity | 10% | Production Well Radius | 707 m |
| NaCl Concentration | 20% | Number of grid cells, vertical | 42 |
| Geothermal Gradient | 35 °C/km | Number of grid cells, horizontal | 117 |
| Surface Temperature | 15 °C | | |
| Reservoir Thickness | 300 m | **Shallow Reservoir** | |
| Rock Density | 2650 kg/$m^3$ | Mean Reservoir Depth | 1.5 km |
| Rock Specific Heat | 1000 J/kg/°C | Mean Reservoir Temperature | 67.5 °C |
| Simulated Radius | 100 km | Well Radius | 400 m |
| Initial Conditions | Hydrostatic equilibrium, pore space occupied by brine | Number of grid cells, vertical | 34 |
| | | Number of grid cells, horizontal | 121 |

#### 3.1.1 Deep Reservoir

The deep reservoir is the thermal source of the CPGES system, providing the heat which is converted to electricity at the surface, shown in Figure 1. To extract heat, $CO_2$ is injected in a cold, supercritical state at the injection well during the energy storage mode. The injection well is located at the bottom of the reservoir, just above the base rock at a radius of 200 meters. Unlike previous models, a horizontal injection well is used instead of a vertical well to increase the $CO_2$ injection area, thereby reducing the pressure losses. The increased well length is particularly critical for the diurnal cycle, where the injection mass flow rate is twice as high as the produced mass flow rate. The injection well is located at the bottom of the reservoir to allow the buoyant $CO_2$ to sweep a majority of the reservoir rock. As the $CO_2$ moves away from the injection well, it extracts heat from the rock, buoyantly rising, until it is captured beneath the caprock. During the generation mode, $CO_2$ is produced from the reservoir at the horizontal-circular production well which is located directly beneath the caprock at the top of the reservoir, at a radius of 707 meters. The radius of the production well corresponds with previous CPG simulations (Adams et al. 2014, 2015; Garapati et al. 2015).

The deep reservoir is initially filled with brine and is primed with $CO_2$ for 2.5 years. The injection rate is linearly ramped over the first year, increasing to 250 kg/s. Thereafter, it is constantly injected at 250 kg/s. During the priming period, 15.78 Mt of $CO_2$ are injected into the deep reservoir, with a final $CO_2$ gas saturation over 30% at the production well. This results in greater than 94% $CO_2$ mass fraction when production begins. After the development period, the intermittent operation of the generation and storage modes begins.

#### 3.1.2 Shallow Reservoir

The shallow reservoir is used to store $CO_2$ produced during the generation mode, which is different from the deep reservoir, which is used to extract heat from the subsurface. In the shallow reservoir, a single well, which functions for both injection and production of $CO_2$, referred to as a "Huff and Puff" method, was selected to minimize the amount of $CO_2$ required to operate the reservoir and reduce the amount of $CO_2$ which is lost into the reservoir, due to advection and diffusion of the $CO_2$ plume. The single well is located at the top of the reservoir directly beneath the caprock at a radius of 400 meters. The placement of the well at the top of the reservoir limits the vertical movement of the buoyant $CO_2$, only allowing the horizontal expansion of the $CO_2$ plume and $CO_2$ diffusion into the brine, thereby retaining the $CO_2$ plume near the well.

Similar to the deep reservoir, the shallow reservoir is initially filled with brine and requires the $CO_2$ plume to be developed prior to the operation of the CPGES system. 1.56 Mt of $CO_2$ are injected over 12 weeks. The $CO_2$ is linearly ramped up from zero to 100 kg/s over two weeks and then remains constant for the remaining 10 weeks. This plume development was needed to limit the amount of brine that is produced from the reservoir during the storage mode. As the CPGES system is regularly operated, the $CO_2$ plume will disperse, due to the $CO_2$ buoyancy and diffusion into the brine. Thus, the shallow reservoir retains 5% of the injected $CO_2$ during each cycle to maintain the $CO_2$ plume.

### 3.2 Surface Modeling

The surface model includes the vertical wells, turbine, pump, throttling valves, and cooling towers. The surface model is numerically coupled with the reservoir model at the injection and production well by the reservoir pressures from the TOUGH2 models.

The vertical well model has been previously documented (Adams et al. 2015) and is briefly summarized here. The vertical well is numerically integrated over 100-meter elements, solving the continuity, energy balance, and momentum equations, neglecting the kinematic effects in the energy equation. Each element is assumed to be adiabatic (Randolph et al. 2012), and pipe friction is modeled using the Darcy-Weisbach relation, assuming a surface roughness of 55 µm (Farshad and Rieke 2006). To reduce pressure losses, each horizontal well is connected to the surface by four vertical wells.

At the surface, $CO_2$ is expanded in the turbine produce power, given as,

$$\dot{E}_{turbine} = \dot{m}_{generation}(h_2 - h_3), \tag{1}$$

where $\dot{m}_{generation}$, $\dot{E}_{turbine}$, and $h$ are the mass flow rate during the generation mode, the power produced by the turbine, and the enthalpy of the fluid, respectively. Enthalpy state points are defined in Figure 1. The turbine outlet enthalpy, $h_3$, is calculated with an isentropic efficiency of 78%, consistent with previous CPG models (Adams et al. 2014, 2015). The turbine back pressure is 7.5 MPa to maintain the produced $CO_2$ in supercritical state and to prevent multiphase $CO_2$ from entering the vertical well at state point 4.

The circulation pump, which is used during the storage mode, consumes power, defined as,

$$\dot{E}_{pump} = \dot{m}_{storage}(h_9 - h_8), \tag{2}$$

where $\dot{E}_{pump}$, $\dot{m}_{storage}$, and $h$ are the pumping power, the mass flow rate during the storage mode, and the enthalpy, respectively. The circulation pump outlet enthalpy, $h_9$, is calculated using an isentropic efficiency of 90%.

The $CO_2$ is cooled at the surface using cooling towers.

$$\dot{Q}_{cooler,generation} = \dot{m}_{generation}(h_3 - h_4), \tag{3}$$

$$\dot{Q}_{cooler,storage} = \dot{m}_{storage}(h_7 - h_8), \tag{4}$$

where $\dot{Q}_{cooler,generation}$, $\dot{Q}_{cooler,storage}$, $\dot{m}_{generation}$, $\dot{m}_{storage}$, and $h$ represent the heat transfer rate during the generation and storage modes, the mass flow rate during the generation and storage mode, and the enthalpy of the $CO_2$, respectively. The cooling towers must consume power to operate the cooling tower fans. We model this parasitic power consumption as a fraction of the heat transfer rate in the cooling tower, defined as,

$$\dot{E}_{cooler,generation} = \lambda_{generation}\dot{Q}_{cooler,generation}, \tag{5}$$

$$\dot{E}_{cooler,storage} = \lambda_{storage}\dot{Q}_{cooler,storage}, \tag{6}$$

Where $\dot{E}_{cooler}$ and $\lambda$ are the cooling tower power consumption and the cooling tower loss fraction, respectively. The cooling tower loss fraction is a function of the cooling tower approach temperature and the ambient wet bulb temperature, and is defined in Adams et al. (2015) for both cooling and condensing towers.

The surface throttling valves, which can replace the cooling tower in the generation mode or the pump in the storage mode, is modeled as an isenthalpic process.

### 3.3 System Performance

The net power that is produced during the generation mode is defined as the difference between the turbine power and the generation cooling tower consumption, given as,

$$\dot{E}_{net,generation} = \dot{E}_{turbine} - \dot{E}_{cooling,generation}, \tag{7}$$

where $\dot{E}_{net,generation}$ is the net power that is produced during the generation mode. The net energy produced during the generation mode is the integral of the net power generated over the duration of the generation mode, defined as,

$$E_{generation} = \int_0^{t_{generation}} \dot{E}_{net,generation}dt, \tag{8}$$

where $E_{generation}$ and $t_{generation}$ are the net energy generated by the system during the generation mode and the duration of the generation mode, respectively.

Similarly, the net power consumed during the storage phase is defined as the sum of the power consumed by the cooling towers and the pump, defined as,

$$\dot{E}_{storage} = \dot{E}_{pump} + \dot{E}_{cooling,storage}, \tag{9}$$

where $\dot{E}_{storage}$ is the total power consumed during the storage mode. The net energy consumed by the system during the storage phase is found by integrating the total power consumed over the duration of the storage mode, given as,

$$E_{storage} = \int_0^{t_{storage}} \dot{E}_{storage}dt, \tag{10}$$

where $E_{storage}$ and $t_{storage}$ are the net energy consumed during the storage phase and the duration of the storage mode, respectively.

The net energy that is produced by the system is defined as the difference between the generated energy during the generation mode and the energy consumed during the storage mode, given as,

$$E_{Net} = E_{net,generation} - E_{storage}, \tag{11}$$

where $E_{Net}$ is the net energy that is produced by the system over a complete generation and storage cycle.

We define the energy storage performance of the CPGES system using the energy storage ratio as the ratio of the net energy generated during the production mode divided by the net power consumed during the storage mode,

$$\chi = \frac{E_{net,generation}}{E_{storage} + Q_{purchased}}, \tag{12}$$

where $\chi$ and $Q_{purchased}$ are the Energy Storage Ratio and the additional surface heating during the power generation mode. The CPGES system does not require additional surface heating to increase the temperature of the fluid prior to the turbine. This differs from compressed air, which requires additional heat, typically from purchased fossil fuels, to produce power during the generation mode.

## 4. RESULTS

We demonstrate how the CPGES system will operate for a diurnal cycle and a biannual cycle. The performance of the system is characterized in terms of the reservoir pressures, component power, net system power, and the energy storage ratio, summarized in Table 2.

The following results occur after ten years of system operation. The diurnal cycle results represent values occurring for a single 24-hour period (i.e. year 10.0000 to 10.0027). Similarly, the seasonal cycle results represent values occurring for a 6-month period after ten years of operation (i.e. year 10.0 to 10.5).

**Table 2: Summary of the key performance characteristics of the CPGES system.**

| Generation Time | Storage Time | Generation Mass Flow Rate (kg/s) | Storage Mass Flow Rate (kg/s) | Generation Average Net Power (MW) | Storage Average Net Power (MW) | Energy Storage Ratio (MW-h/MW-h) |
|---|---|---|---|---|---|---|
| 16 hours | 8 hours | 200 | 380 | 1.63 | 1.11 | 2.93 |
| 16 hours | 8 hours | 300 | 570 | 2.29 | 2.33 | 1.95 |
| 3 months | 3 months | 200 | 190 | 1.50 | 0.99 | 1.55 |
| 3 months | 3 months | 300 | 285 | 1.97 | 1.87 | 1.05 |

Several trends are immediately apparent in the data: the energy storage ratio decreases with increased mass flow rate; the average generation and storage power increases with mass flow rate, and increasing the overall cycle period (i.e. from one day to six months) decreases the energy storage ratio. However, in all cases, the energy storage ratio of the system is still greater than one. Below, we discuss these results in detail.

### 4.1 Diurnal Cycle

The CPGES system can operate on a diurnal cycle, producing and consuming power during a 24-hour period. To simulate a diurnal cycle, the system generates power for 16 hours and stores power for 8 hours. These time periods correlate with periods where the cost of electricity are elevated and reduced (MISO 2016). The storage mass flow rate, listed in Table 2, is selected to retrieve 95% of the $CO_2$ stored in the shallow reservoir back to the deep reservoir. This process continuously deposits small amounts of $CO_2$ into the shallow reservoir to maintain high $CO_2$ saturation near the well, making up for $CO_2$ that has diffused away into the reservoir.

Figure 2 shows the varying reservoir pressures over a 24 hour period (Figure 2A and 2B) and the corresponding power generation and storage (Figure 2C and 2D). Figures 2A and 2C show results for a 200 kg/s generation mass flow rate and Figures 2B and 2D show results for a 300 kg/s generation mass flow rate.

Figure 2A shows the injection of $CO_2$ into each reservoir increases the pressure at each injection well downhole, while the production of $CO_2$ from each reservoir decreases the pressure at each production well downhole. In the deep reservoir, only one of the wells is active during each mode, while the other is stopped. Despite there being no flow in a production or injection well at any given time, the stopped well downhole pressure will vary based on the activity from the other well. Over a complete cycle, the downhole pressure at the deep reservoir varies from 23.01 MPa to 23.57 MPa, and 22.24 MPa to 23.46 MPa for the production well, 26.78 to 28.22 to 26.94 MPa to 28.98 MPa for the injection well, while the shallow reservoir varies from 13.34 MPa to 14.35 MPa, and 13.19 MPa to 14.63 MPa for generation mass flow rates 200 kg/s and 300 kg/s, respectively.

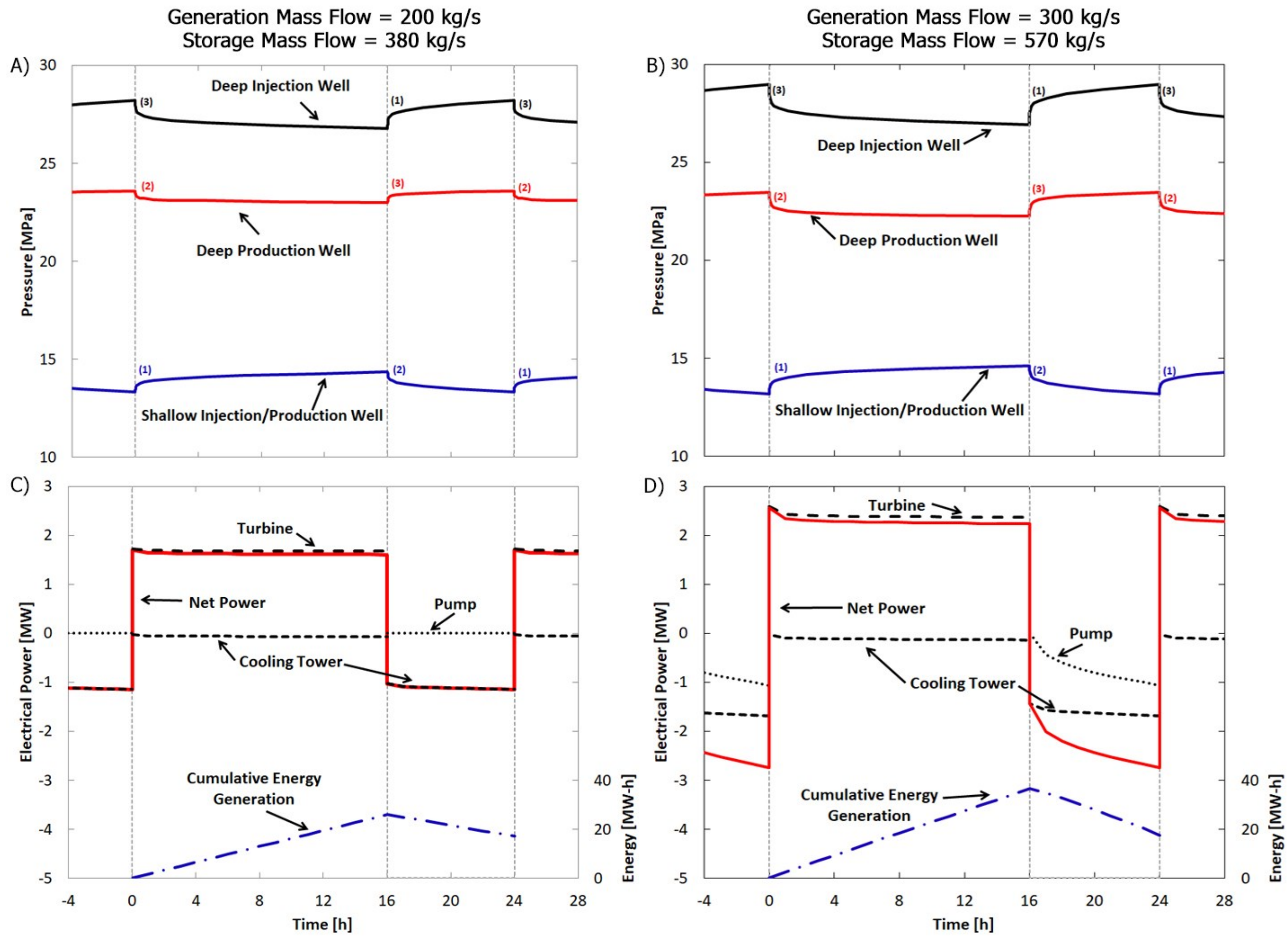


**Figure 2: The transient reservoir (A, B) and power (C, D) performance of the CPGES system for a single diurnal cycle after ten years of intermittent operation for the 200 kg/s (A, C) and 300 kg/s (B, D) mass flow rates cases. The pressure transients result from the mass flow conditions: (1) injection of $CO_2$, (2) production of $CO_2$, and (3) the resting period where no $CO_2$ is injected or produced. The power production and consumption are directly impacted by the reservoir conditions, varying with the reservoir pressures. The system operates in the generation mode for the first 16 hours, followed by the energy storage mode for 8 hours.**

Figure 2C and 2D show the system produces steady power during the generation mode, despite the variation in the reservoir pressures in Figure 2A and 2B. The net power produced varies from 1.71 MW to 1.61 MW for the 200 kg/s generation case (Figure 2C) and 2.57 MW to 2.24 MW for the 300 kg/s generation case (Figure 2D). In both cases, over 60% of the variation in the net power generated occurred within the first hour of operation, due to the large variation in pressure at each well during this time, thus the system generates consistent power for the remaining 15 hours of the generation period.

Alternatively, the power consumed during the storage period is steady only for the 380 kg/s storage case (Figure 2C) but continuously increases for the 570 kg/s storage case (Figure 2D). This difference is a result of operating the pump, which is required in the 570 kg/s case. For the storage mass flow rate of 380 kg/s, the pump is not required during the storage mode, and the power is consumed by the cooling towers, which increase from 1.03 MW to 1.14 MW over the 8 hours of the storage mode. In the case with the 570 kg/s storage mass flow rate, pumping is required and the power stored increases from 1.43 MW to 2.74 MW over the duration of the mode, with the cooling towers increasing from 1.43 MW to 1.68 MW while the pump increases from 0 MW to 1.06 MW. Thus, the majority of the storage power increase is caused by the required pumping.

Normally, the injection temperature of the $CO_2$ is used to control the downhole pressure. As the injection temperature decreases, the density increases, and therefore the downhole pressure, which is the product of density, gravitational constant, and reservoir depth, also increases. However, the injection temperature is limited by the sum of the ambient temperature and the approach temperature, thereby limiting this pressure rise that can be achieved by gravitational compression. Thus, for this 570 kg/s case (Figure 2D), the pump is used to increase the injection pressure beyond what can be achieved by gravitational compression alone. Over the duration of the storage mode, the downhole injection pressure increases as $CO_2$ is injected, therefore pump power will always rise when pumping is required in the storage mode.

The net energy produced during the generation mode increases from 25.99 MW-h to 36.47 MW-h when the generation mass flow rate increases from 200 kg/s to 300 kg/s, while the amount of energy consumed during the storage mode increases from 8.89 MW-h to 18.85 MW-h. Despite these differences, both cases have similar net daily energy generation, with the 200kg/s and 300 kg/s cases producing 17.1 MW-h and 17.6 MW-h, respectively. The resulting energy storage ratios are 2.93 and 1.95 for the 200 kg/s and 300 kg/s generation cases, respectively. The system operates with an energy storage ratio greater than one, meaning the energy generated by the system was greater than the energy that was stored. This occurs because the system operates both as a geothermal electricity plant and an energy storage plant. Thus, the additional power generated is produced from the geothermal heat input from the deep reservoir.

The similar daily generation values of 17.1 MW-h and 17.6 MW-h are due to the 112% increase in pumping required from the 200 kg/s to the 300 kg/s generation case, while the power generation only increased by 40%. For further increases in mass flow rate, it is expected that the power consumed by the pump will increase at a greater rate than the power generated, resulting in an "optimal" mass flow rate at the peak of net daily energy generation, similar to the CPG system (Adams et al. 2015). For this configuration, this maximum net daily energy occurs at a mass flow rate between the 200 kg/s and 300 kg/s generation cases.

While the net daily energy generation can be maximized, the system may be operated to maximize different quantities. For example, the magnitude of energy generated and stored will continue to increase with increasing mass flow rates, despite a decreasing net energy produced. Thus, if the prices of electricity during storage and generation modes are sufficiently extreme, the system may be operated at higher mass flowrates, decreasing overall net energy produced, but maximizing revenue.

### 4.2 Seasonal Cycle

The period of storage for a CPGES system is not limited to a 24-hour period. CPGES may be used to store energy for weeks or months when electricity is expensive and later generate when prices decline. Therefore, to illustrate the variable-term energy storage potential of the CPGES system, we demonstrate the operation of a system at the long-term extreme, a biannual or seasonal cycle. This seasonal system operates using the same parameters and configuration of the diurnal cycle; however, we simulate continuous generation for 3-months followed by continuous storage for 3-months.

Figure 3 shows the variation in reservoir pressures for the 200 kg/s (Figure 3A) and the 300 kg/s (Figure 3B) generation mass flow rates. The instantaneous electric power and cumulative energy generated are shown for the 200 kg/s (Figure 3C) and 300 kg/s (Figure 3D) generation mass flow rates. The duty cycle of this seasonal system is 50%, unlike the 67% duty cycle of the diurnal system; thus, the storage mass flow rate is only 95% of the generation flow rate.

Figures 3A and 3B show the variation in the downhole pressure at each well is greater than the diurnal cycle, due to the larger volume of $CO_2$ that is injected or removed from each reservoir. For example, in the 200 kg/s generation mass flow rate case (Figure 3A), the pressure varies between 21.3 MPa and 25.5 MPa for the deep production well, compared to 23.0 MPa and 23.6 MPa in the diurnal cycle. Similarly, in the 300 kg/s generation mass flow rate case (Figure 3B) the downhole pressure varies between 18.8 MPa and 26.8 MPa, compared to 22.4 and 23.5 MPa in the diurnal cycle. This large variation in pressure causes a corresponding variation in the power generation or consumption in each case.

Figure 3C and 3D show the instantaneous power generation decreases over the course of the generation period from 1.97 MW to 1.46 MW for a mass flow rate of 200 kg/s (Figure 3C), and 3.21 MW to 0.95 MW for a 300 kg/s mass flow (Figure 3D). This decrease in power generation occurs as a result of two factors: a decrease in turbine power due to the pressure drawdown of the deep reservoir at the production well, and an increase in the cooling tower power, due to a downhole pressure rise in the shallow reservoir. Over the course of the generation mode, the system generates 3.34 GW-h and 4.31 GW-h of energy for the 200 kg/s and 300 kg/s generation cases, respectively. When considered over 3 months of operation, this system generates on average 1.54 MW and 1.57 MW for the 200 kg/s and 300 kg/s cycles, respectively, which are lower than the diurnal cycle values of 1.63 MW and 2.29 MW.

The seasonal cycle differs from the diurnal cycle primarily due to the increased pumping and cooling tower loads during the storage mode, shown as the negative electric power values in Figures 3C and 3D. The amount of power that the system stores increases from 0.33 MW to 1.76 MW between the start and end of the 200 kg/s case, and similarly increases from 0.47 MW to 3.53 MW between the start and end of the 300 kg/s case, storing 2.15 GW-h and 4.09 GW-h over the entire cycle. When considered over the 3 months of operation, this amounts to an average of 0.99 MW and 1.87 MW for the 200 kg/s and 300 kg/s cycles, respectively, which are less than the diurnal cycle average values of 1.11 MW and 2.33 MW. However, due to the variation in the generation duty cycle and the associated change in storage mass flow rate, the seasonal system operates with higher energy consumption per cycle period than the diurnal, even though the instantaneous power generation is lower than the diurnal cycle.

When the total generation energies are divided by the total storage energies, the seasonal cycle has energy storage ratios of 1.55 and 1.05, for the 200 kg/s and 300 kg/s cases, respectively. These energy storage ratios are significantly lower than the diurnal cycle values of 2.93 and 1.95, due to the increase in the storage energy consumption, the decrease in the generation energy output, and variation in the duty cycle. For example, by the end of the 300 kg/s cycle, the power consumed by the cooling tower exceeded 46% of the total turbine power.

In these seasonal cases, the elevated downhole deep injection well pressure requires larger pump power than the diurnal cases. Over the duration of the three-month storage period, the pump consumes 1.2 GW-h for the 200 kg/s case and 2.67 GW-h for the 300 kg/s case, or 26% and 44%, respectively, of the total energy generated by the turbine. In contrast, the pump consumes 0% and 15% of the total power generated by the turbine the diurnal phase. Thus, the pump operation is a key factor that decreases the energy storage ratio in the seasonal cycle.

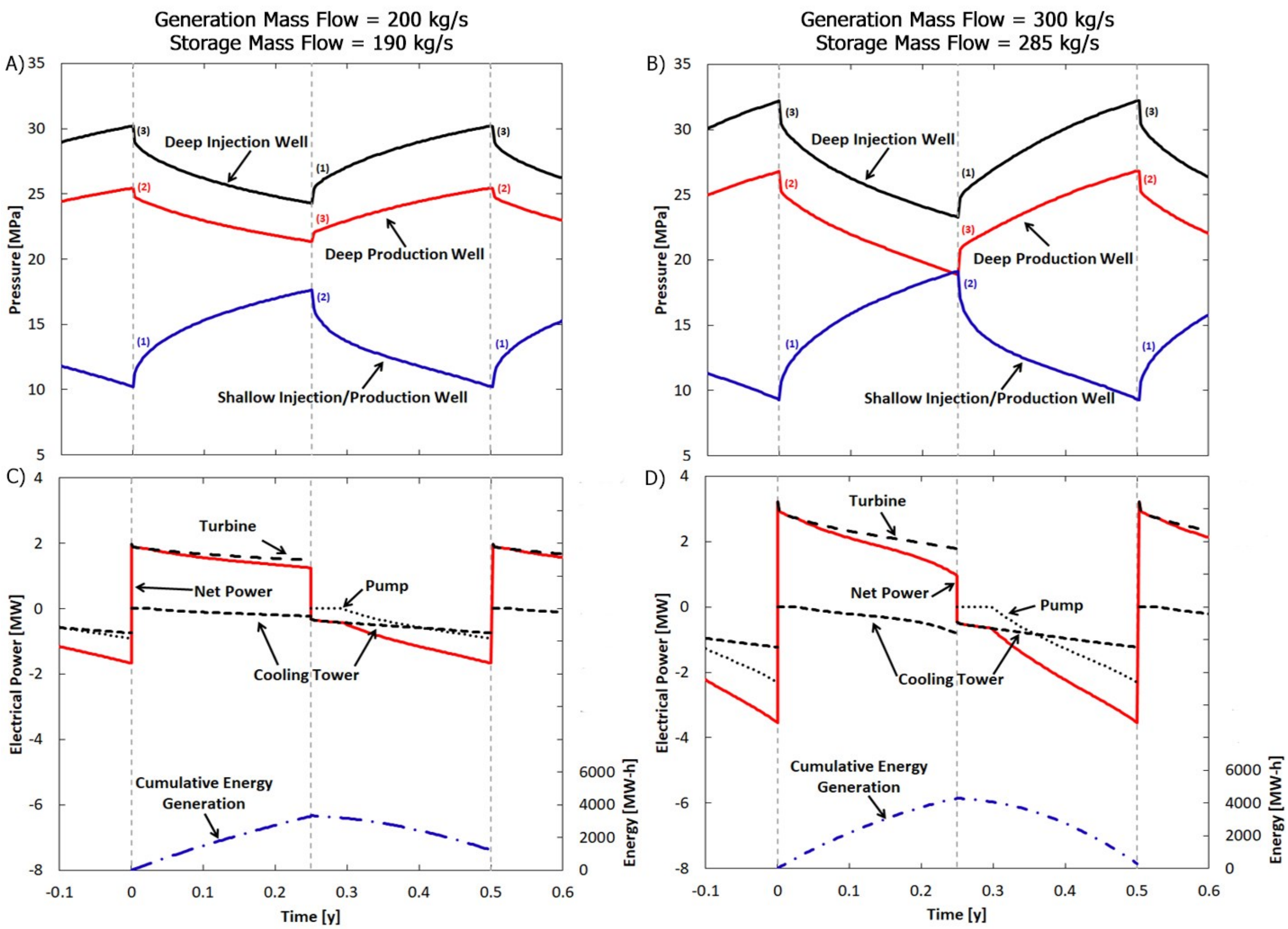


**Figure 3: The pressure (A, B) and power (C, D) performance of the CPGES system for the long-term storage cycle for a single cycle for the 200 kg/s (A, C) and 300 kg/s (B, D) mass flow rates. The system is illustrated after 10 years of energy storage operation. The pressure transients result from the mass flow conditions: (1) injection of $CO_2$, (2) production of $CO_2$, and (3) the resting period where no $CO_2$ is injected or produced. The power transients result from the variation in the reservoir pressures at each well, which results from the intermittent injection and/or production of $CO_2$ in the reservoir.**

While the elevated storage-phase power (i.e. cooling tower and pump) accounts for most of the decrease in energy storage ratios of the seasonal system, the non-zero cooling tower power during the generation phase also contributes to this decrease. The energy storage ratio of the CPGES system can be greater than zero because the components which generate the power (i.e. turbine) can be temporally offset from the components which consume power (i.e. cooling towers and pumps). When some power consumption is needed during the generation mode, as occurs in the 300 kg/s case (Figure 3D), this reduces the decoupling of generation and consumption components, decreasing the energy storage ratio. One option that could be used to reduce the generation phase cooling tower power consumption would be a significantly larger well radius in the shallow reservoir. The large radius would increase the accessible volume which would decrease the reservoir pressure, reduce the required pre-injection cooling, and ultimately increase the energy storage ratio.

## 5. IMPLICATIONS

The CPGES system can operate over a range of energy storage cycle durations, as demonstrated in this paper in terms of a diurnal and biannual (seasonal) cycle, which illustrate a range of cycle durations that are more than sufficient to provide full storage support to variable renewable sources, thereby allowing for increased renewable energy penetration into the electrical grid. While the pressure transients affect the power generation and storage over the course of the cycle, the ultimate limitation of the cycle duration is the size of the $CO_2$ plume in the reservoir, and given the large volume of $CO_2$ that is required to mitigate climate change, the operation of the system could be substantially longer than the simulated cycle times. This ability to operate over extended cycle durations, is an advantage that CPGES has over existing storage systems, such as compressed air, which can only generate power over limited periods, typically a few hours, before the system must be recharged.

The CPGES system operates using only geothermal resources, requiring no additional fuel sources at the surface, while providing permanent subsurface storage for $CO_2$. This allows the CPGES system to supplement variable renewable sources using renewable energy to provide baseload power, which is not achieved using existing energy management practices, which generally use fossil fuels, typically natural gas, to supplement wind and solar sources, which increase the carbon cost of operating these systems to provide baseload power. Furthermore, beyond providing renewable energy, the CPGES system has the synergistic effect of reducing the environmental impact of nearby $CO_2$ sources by permanently capturing $CO_2$ in the surface, thereby reducing the amount of $CO_2$ emitted into the atmosphere.

The amount of power that can be produced can be increased by operating over a larger subsurface area, scaling up the power production and consumption, similar to the approach applied to the CPG system (Bielicki et al. 2016).

## 6. CONCLUSION

A CPG system can be modified to operate as an energy storage system, CPGES, to temporally separate the power generation and power consumption components in a power cycle. System modeling of CPGES allows for the following conclusions:

*A second, shallow reservoir can be added to the CPG system to separate power generation and energy storage.* The second reservoir stores the $CO_2$ in an intermediate state after it is expanded in the turbine before the parasitic cooling and pump loads. Later, the $CO_2$ is re-extracted where it is cooled and compressed, consuming power before it is injected into the deep reservoir. Thus, the shallow reservoir allows the turbine to be separated from the consumptive elements of the power cycle, allowing for intermittent operation.

*The shallow reservoir can operate with a single well, which operates as both the production and injection well for the system*. The shallow reservoir operates as an intermediate storage vessel for the $CO_2$ between the generation and storage modes. The injected $CO_2$ must be stored adiabatically and then later recovered for the energy storage process to function. A single horizontal circular injection well placed directly beneath the caprock and a continuous sequestration of 5% of the $CO_2$ allowed the majority injected $CO_2$ to be recovered with minimal brine entrainment.

*The energy storage system produces net positive energy to the grid*. The system operates with an energy storage ratio greater than one for both the diurnal and seasonal cases. The diurnal case can operate with an energy storage ratio of 2.93, meaning it produces almost three times more power during the generation phase than it stores in the storage phase. The system is able to produce significantly more power than it stores due to the geothermal heat from the deep reservoir. The seasonal energy storage system operates with an energy storage ratio of 1.55, which is lower than the diurnal cycle value of 2.93, a result of the larger pressure oscillations in the reservoir. The minimum energy storage ratio was 1.05 for the 300 kg/s seasonal storage case, due to larger than optimal mass flowrates in the generation period; however, this system still generated more electric output than it stored.

*The system can operate over a range of cycle durations, providing a robust energy storage solution.* The system was demonstrated operating on both a diurnal and a biannual cycle, while still producing net energy to the grid. Thus, the system is not limited to a given cycle length and can operate over any cycle duration that may be required to supplement variable renewable sources.

## ACKNOWLEDGEMENTS

We gratefully acknowledge funding from the National Science Foundation (NSF) under the Sustainable Energy Pathways (SEP) grant number SEP-1230691 and from the George and Orpha Gibson endowment for Prof. Saar's Hydrogeology and Geofluids research group in the Department of Earth Sciences at the University of Minnesota (UMN). We would also like to thank the Initiative for Renewable Energy and the Environment (IREE), a signature program of the Institute on the Environment (IonE) at the University of Minnesota. We also acknowledge funding from ETH Zurich (ETHZ) and from the Werner Siemens-Stiftung/Foundation (WSS) for Prof. Saar's Geothermal Energy and Geofluids Group at ETH Zurich, Switzerland. Any opinions, findings, conclusions, or recommendations in this paper are those of the authors and do not necessarily reflect the views of the NSF, UMN, IREE, IonE, ETH, or WSS.

Disclaimer: Dr. Saar and Dr. Randolph have a significant financial interest and a business interest, in TerraCOH Inc., a company that may commercially benefit from the results of this research. The University of Minnesota has the right to receive royalty income under the terms of a license agreement with TerraCOH Inc. These relationships have been reviewed and managed by the University of Minnesota in accordance with its conflict of interest policies.

## REFERENCES

Adams, B. M., Kuehn, T. H., Bielicki, J. M., Randolph, J. B., & Saar, M. O. (2014). On the importance of the thermosiphon effect in CPG (CO2 plume geothermal) power systems. *Energy*, *69*, 409–418. doi:10.1016/j.energy.2014.03.032

Adams, B. M., Kuehn, T. H., Bielicki, J. M., Randolph, J. B., & Saar, M. O. (2015). A comparison of electric power output of CO2 Plume Geothermal (CPG) and brine geothermal systems for varying reservoir conditions. *Applied Energy*, *140*, 365–377. doi:10.1016/j.apenergy.2014.11.043

Atrens, A. D., Gurgenci, H., & Rudolph, V. (2009). CO2 Thermosiphon for competitive geothermal power generation. *Energy and Fuels*, *23*(1), 553–557. doi:10.1021/ef800601z

Atrens, A. D., Gurgenci, H., & Rudolph, V. (2010). Electricity generation using a carbon-dioxide thermosiphon. *Geothermics*, *39*(2), 161–169. doi:10.1016/j.geothermics.2010.03.001

Bielicki, J. M., Adams, B. M., Choi, H., Jamiyansuren, B., Saar, M. O., Taff, S. J., et al. (2016). Sedimentary Basin Geothermal Resource for Cost-Effective Generation of Renewable Electricity from Sequestered Carbon Dioxide. *41st Stanford Geothermal Workshop*, 1–4.

Bird, L., Milligan, M., & Lew, D. (2013). *Integrating Variable Renewable Energy: Challenges and Solutions*. *NREL/TP-6A20-60451*.

doi:NREL/TP-6A20-60451

Brown W., D. (2000). A Hot Dry Rock Geothermal Energy Concept Utilizing Supercritical CO2 Instead of Water. In *Twenty-Fifth Workshop on Geothermal Reservoir Engineering* (Vol. 1995, pp. 1–6). Stanford, California, California. doi:10.1016/j.apenergy.2014.02.027

Buscheck, T. A., Bielicki, J. M., Edmunds, T. A., Hao, Y., Sun, Y., Randolph, J. B., & Saar, M. O. (2016). Multifluid geo-energy systems: Using geologic CO2 storage for geothermal energy production and grid-scale energy storage in sedimentary basins. *Geosphere*, *12*(3), 678–696. doi:10.1130/GES01207.1

EIA. (2017). Electric Power Monthly. *Electric Power Monthly*. https://www.eia.gov/electricity/monthly/epm_table_grapher.php?t=epmt_6_07_b. Accessed 11 January 2017

Farshad, F., & Rieke, H. (2006). Surface-Roughness Design Values for Modern Pipes. *SPE Drilling & Completion*, *21*(3), 2004–2007. doi:10.2118/89040-PA

Garapati, N., Randolph, J. B., & Saar, M. O. (2015). Brine displacement by CO2, energy extraction rates, and lifespan of a CO2-limited CO2-Plume Geothermal (CPG) system with a horizontal production well. *Geothermics*, *55*, 182–194. doi:10.1016/j.geothermics.2015.02.005

Garapati, N., Randolph, J. B., Valencia, J. L., & Saar, M. O. (2014). CO2-plume geothermal (CPG) heat extraction in multi-layered geologic reservoirs. *Energy Procedia*, *63*, 7631–7643. doi:10.1016/j.egypro.2014.11.797

IPCC. (2014a). *Climate Change 2014: Mitigation of Climate Change. Working Group III Contribution to the Fifth Assessment Report of the Intergovernmental Panel on Climate Change*. *Working Group III Contribution to the Fifth Assessment Report of the Intergovernmental Panel on Climate Change*. Cambridge: Cambridge University Press. doi:10.1017/CBO9781107415416

IPCC. (2014b). *Climate Change 2014: Synthesis Report. Contribution of Working Groups I, II and III to the Fifth Assessment Report of the Intergovernmental Panel on Climate Change*. doi:10.1017/CBO9781107415324

Klein, S., & Alvarado, F. (2002). Engineering Equation Solver. *F-Chart Software*. F-chart.

Koohi-Kamali, S., Tyagi, V. V., Rahim, N. A., Panwar, N. L., & Mokhlis, H. (2013). Emergence of energy storage technologies as the solution for reliable operation of smart power systems: A review. *Renewable and Sustainable Energy Reviews*, *25*, 135–165. doi:10.1016/j.rser.2013.03.056

Liu, H., He, Q., Borgia, A., Pan, L., & Oldenburg, C. M. (2016). Thermodynamic analysis of a compressed carbon dioxide energy storage system using two saline aquifers at different depths as storage reservoirs. *Energy Conversion and Management*, *127*, 149–159. doi:10.1016/j.enconman.2016.08.096

Metz, B., Davidson, O., de Coninck, H., Loos, M., & Meyer, L. (2005). *Carbon Dioxide Capture and Storage*. *Intergovernmental Panel on Climate Change* (Vol. 2). doi:10.1002/anie.201000431

MISO. (2016). Midcontinent Independent System Operator Market Reports. https://www.misoenergy.org/Library/MarketReports/Pages/MarketReports.aspx. Accessed 4 May 2016

Phuangpornpitak, N., & Tia, S. (2013). Opportunities and challenges of integrating renewable energy in smart grid system. *Energy Procedia*, *34*, 282–290. doi:10.1016/j.egypro.2013.06.756

Pruess, K. (2005). *ECO2N: A TOUGH2 Fluid Property Module for Mixtures of Water, NaCl, and CO2*.

Pruess, K. (2008). On production behavior of enhanced geothermal systems with CO2 as working fluid. *Energy Conversion and Management*, *49*(6), 1446–1454. doi:10.1016/j.enconman.2007.12.029

Pruess, K., Oldenburg, C., & Moridis, G. (2012). *TOUGH2 User's Guide*. *Report LBNL-43134, Lawrence Berkeley National Laboratory, California*.

Randolph, J. B., Adams, B. M., Kuehn, T. H., & Saar, M. O. (2012). Wellbore Heat Transfer in CO2-based Geothermal Systems. In *Geothermal Resources Council Transaction* (Vol. 36).

Randolph, J. B., & Saar, M. O. (2011a). Combining geothermal energy capture with geologic carbon dioxide sequestration. *Geophysical Research Letters*, *38*(10), n/a-n/a. doi:10.1029/2011GL047265

Randolph, J. B., & Saar, M. O. (2011b). Impact of reservoir permeability on the choice of subsurface geothermal heat exchange fluid: CO2 versus water and native brine. In *Proceedings for the geothermal resources council 35th annual meeting* (Vol. 38, pp. 23–26).

Randolph, J. B., & Saar, M. O. (2011c). Coupling carbon dioxide sequestration with geothermal energy capture in naturally permeable, porous geologic formations: Implications for CO2 sequestration. *Energy Procedia*, *4*, 2206–2213. doi:10.1016/j.egypro.2011.02.108

Sørensen, B. (2015). *Solar energy storage*. Elsevier.

United Nations Framework Convention on Climate Change. (2015). *Paris Agreement* (No. 21932). *Conference of the Parties on its twenty-first session*. Paris. doi:FCCC/CP/2015/L.9/Rev.1